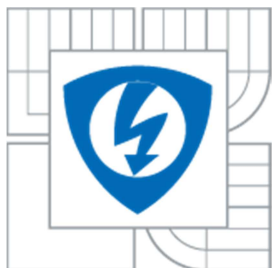




VYSOKÉ UČENÍ TECHNICKÉ V BRNĚ

BRNO UNIVERSITY OF TECHNOLOGY



FAKULTA ELEKTROTECHNIKY A KOMUNIKAČNÍCH  
TECHNOLOGIÍ

ÚSTAV FYZIKY

FACULTY OF ELECTRICAL ENGINEERING AND COMMUNICATION  
DEPARTMENT OF PHYSICS

## NOISE AND TRANSPORT ANALYSIS OF THE NIOBIUM OXIDE LAYERS

ANALÝZA TRANSPORTNÍCH A ŠUMOVÝCH CHARAKTERISTIK OXIDOVÝCH VRSTEV NA BÁZI  
NIOBU

### ZKRÁCENÁ VERZE DOKTORSKÉ PRÁCE

SHORTENED VERSION OF DOCTORAL THESIS

AUTOR PRÁCE

**RNDr. ZDENĚK SITA**

AUTHOR

VEDOUCÍ PRÁCE

Prof. Ing. LUBOMÍR GRMELA, CSc.

SUPERVISOR

**BRNO 2015**

## **Keywords**

Niobium oxide capacitor, MIS structure, charge carrier transport, niobium pent-oxide, Volt-Ampere characteristics, capacitance of depleted layer, noise

## **Klíčová slova**

Niobové kondenzátory, MIS struktura, transport nosičů náboje, oxid niobičný, voltampérové charakteristiky, kapacita ochuzené vrstvy, šum

SITA, Z. *Noise and transport analysis of the Niobium oxide layers*. Lanškroun: University of technology Brno, Faculty of electrical engineering and communication, 2015. 109 p. Supervisor prof. Ing. Lubomír Grmela, CSc.

SITA, Z. *Analýza transportních a šumových charakteristik oxidových vrstev na bázi niobu*. Lanškroun: Vysoké učení technické v Brně, Fakulta elektrotechniky a komunikačních technologií, 2015. 109 s. Vedoucí práce prof. Ing. Lubomír Grmela, CSc.

## Content

1. INTRODUCTION .....	5
2. STATE-OF-THE-ART .....	5
2.1 Technology of solid electrolytic capacitor production .....	5
2.2 COMPARISON of Niobium Oxide and tantalum capacitors .....	6
2.3 Dielectric of NbO capacitor .....	7
2.4 Carrier transport mechanism .....	9
2.4.1 V-A characteristics.....	9
2.4.2 Potential barriers and capacitance.....	11
2.4.3 Activation energy of leakage current .....	11
2.4.4 Fast and slow energy localized states.....	12
2.4.5 Noise.....	12
3. AIM OF DISSERTATION.....	14
4. EXPERIMENTAL PART .....	15
4.1 Study of basic parameters of the band diagram .....	15
4.1.1 Tested samples .....	15
4.1.2 Testing methods.....	15
4.1.3 V-A characteristics.....	15
4.1.4 V-A characteristics in reverse mode .....	15
4.1.5 Fitting of V-A characteristics.....	15
4.1.6 Capacitance of depleted layer.....	17
4.1.7 Temperature dependence of leakage current.....	18
4.1.8 Time dependence of leakage current during charging and discharging .....	18
4.1.9 Restoring voltage of NbO capacitors.....	19
4.1.10 Noise.....	20
4.2 Improvement of the technology .....	21
4.2.1 Comparison of Nb and NbO technology.....	21
4.2.2 NbO powders with various parameters .....	22
4.2.3 Stability of doped powder .....	23
4.2.4 Dielectric's cleaning .....	23
4.2.5 Anodic oxidation improvement .....	24
4.2.6 Correlation of transport parameters with reliability.....	25
5. CONCLUSIONS .....	27
6. LITERATURE.....	28



# 1. INTRODUCTION

Increased demand for tantalum capacitors at the end of last millennium accelerated the search for new technologies, which were able to solve the weak points of tantalum technology – limited source chain, tantalum cost and its susceptibility to thermal runaway failures. Niobium oxide capacitors were developed by J.Fife et al. from AVX, who realized that the conductivity of niobium monoxide is sufficient to be used as an anode, whereas anodization provides even higher quality dielectrics than that of Niobium metal.

Structure of the solid electrolytic capacitor can be understood as a reverse MIS structure, where Metal is the anode, Insulation layer is the metal oxide dielectrics and Semiconductor is the solid electrolyte. Study of charge carrier transport in the Nb<sub>2</sub>O<sub>5</sub> dielectrics of Niobium Monoxide (further „NbO“) capacitor is a subject of this work. The aim is to characterize the active region quality of NbO capacitors based on evaluation of volt-ampere, current-time and noise characteristics and their temperature or voltage dependences. The model of MIS structure is utilized in order to provide a physical interpretation of transport phenomena in the capacitor.

## 2. STATE-OF-THE-ART

### 2.1 TECHNOLOGY OF SOLID ELECTROLYTIC CAPACITOR PRODUCTION

Tantalum and NbO solid electrolytic capacitors are manufactured by similar process from a very pure raw powder with particle size 0.5 to 40µm, depending on the application voltage and requested capacitance [1]. The powder is mixed with a binder and resulting granulate is compressed with high pressure around the Tantalum wire to produce an anode. The anode is then sintered at high temperatures between 1400-1800°C in deep vacuum, where individual particles are sintered to form a sponge-like structure with high volumetric efficiency and surface.

Dielectric is formed electrochemically by anodic oxidation of Ta or NbO anode. Metal pent-oxide is formed in a weak acid at elevated temperature. The interface between oxide and electrolyte is a crucial region for anodic oxidation. At the NbO - dielectrics interface an oxidation takes place and create a transition region of sub-oxides. As a result of several stable Niobium oxide forms the structure of the dielectrics on the boundary gradually changes from the NbO mon-oxide to the fully saturated Nb<sub>2</sub>O<sub>5</sub> pent-oxide. Transition region of sub-oxides has approximately 2nm [2]. Oxide layer thickness is proportional to forming voltage. Niobium pent-oxide is thicker because anodization coefficient is higher in proportion of dielectric constants.

Dielectrics thickness is controlled by current and voltage, applied during the formation process. At first part of anodization process, constant current is held and voltage is increased until the target voltage is achieved. Voltage determines the thickness of the dielectrics. The power supply is then switched to constant voltage to form a homogenous dielectrics thickness all over the dielectrics.

The second electrode (cathode) is prepared by dipping of the anodized pellet into manganese nitrate and by subsequent pyrolysis at 250°C under controlled humidity. Dipping is repeated several times, first to the diluted nitrate solution to achieve good penetration into the sponge-like anodized pellet, later to dense slurry to provide a good overcoat on the top of the pellet. Typically 20 dips are needed to form a high quality electrode [1]. Additional re-forming steps at 40% of original forming voltage are inserted between selected dipping steps to improve the dielectrics quality.

The impregnated pellet is then dipped to graphite dispersion and later to silver loaded epoxy dispersion, and both materials are cured at 150-200°C. The graphite layer is used to create an ohmic contact of silver with manganese dioxide. The top silver layer provides good transport of charge to the cathode electrode. The silvered pellet is assembled to the anode terminal leadframe by silver loaded epoxy glue and the wire is welded to the cathode terminal of the leadframe. The whole assembly is encapsulated to the silica filled epoxy case – see *Fig. 1*.

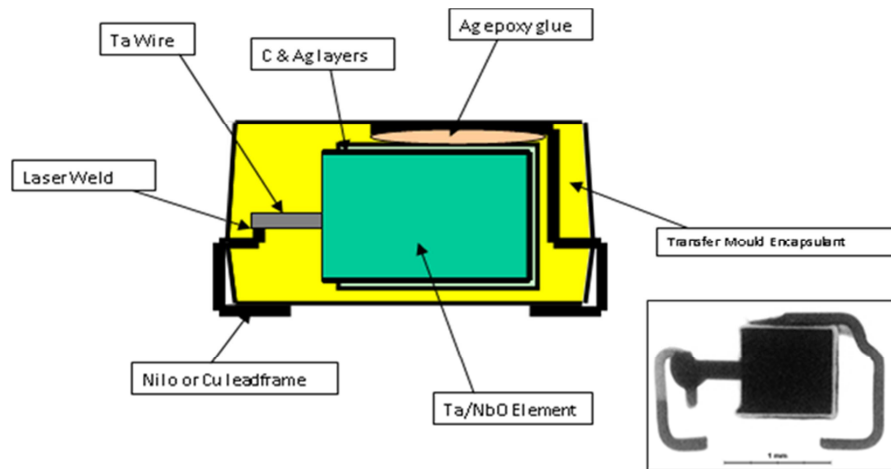


*Fig.1. Final assembly of Ta and NbO capacitor*

## 2.2 COMPARISON OF NIOBIUM OXIDE AND TANTALUM CAPACITORS

Niobium oxide and Tantalum capacitors are in principle similar. Both Tantalum and Niobium elements belong to valve metals, which can be oxidized to highly isolative pent-oxide dielectrics with high dielectric strength. There are however some basic differences.

*Table 1. Difference between Tantalum and Niobium oxide capacitor*

Parameter	Tantalum capacitor	Niobium capacitor
Anodic material	Metal, bcc	Semiconductor, NaCl, oxide deficiency creates conductive band
Anode surface	Thin passivation oxide	Mon-oxide with thin passivation of high oxides
Oxide dielectric constant	27	42
Dielectric growth rate	1,7nm/V	2,5nm/V
Stable sub-oxides	Ta <sub>2</sub> O <sub>5</sub>	Nb <sub>2</sub> O <sub>5</sub> , NbO, NbO <sub>2</sub>
Forming ratio	3-3,5	3,5-4
Burning rate	10,5mm/s	1,5m/s
Self-healing process	MnO <sub>2</sub> - >Mn <sub>2</sub> O <sub>5</sub>	1. MnO <sub>2</sub> - >Mn <sub>2</sub> O <sub>5</sub> 2. NbO->NbO <sub>2</sub>
Volumetric efficiency	100kμFV/g	50kμFV/g
Max. rated voltage	50V	16V
Leakage current spec	1% CxV	2%Cx2
Reliability	1%/1000hrs	1%/1000hrs

### 2.3 DIELECTRIC OF NBO CAPACITOR

A model of the MIS structure was proposed by Šikula et. al. with aim to provide physical interpretation of the NbO and Ta capacitor's VA and CV characteristics and their temperature dependences [10-15]. MIS structure of both capacitors consists of the metallic NbO or Ta anode, insulating Nb<sub>2</sub>O<sub>5</sub> or Ta<sub>2</sub>O<sub>5</sub> dielectrics and semiconductor - MnO<sub>2</sub> anode.

Amorphous insulating Nb<sub>2</sub>O<sub>5</sub> or Ta<sub>2</sub>O<sub>5</sub> layers, prepared by anodic oxidation, are not perfect structures, but real films with a three dimensional disordered lattice. An impurity band is created in the amorphous insulating layer due to defects in concentration  $10^{18}$  to  $10^{19}$  cm<sup>-3</sup>. Charge carrier transport is realized by thermally activated electron hopping between the localized states in the impurity band (Poole-Frenkel emission) and electron tunnelling between deep impurity states or to conductive band. MIS structure models of NbO capacitors before and in equilibrium state are shown on *Fig. 2 and 3*.

Leakage current in forward mode is determined by the potential barrier between NbO and Nb<sub>2</sub>O<sub>5</sub>. In reverse mode it is given by the potential barrier between Nb<sub>2</sub>O<sub>5</sub> and MnO<sub>2</sub>. Work function difference between metal and semiconductor electrode is the reason, why Tantalum and NbO capacitors have non-symmetric VA characteristics and why they are unipolar components. The height of barriers defines maximal usable voltage, which can be applied to the capacitor in the forward and reverse mode. It is a material constant, but it can be improved by used technology.

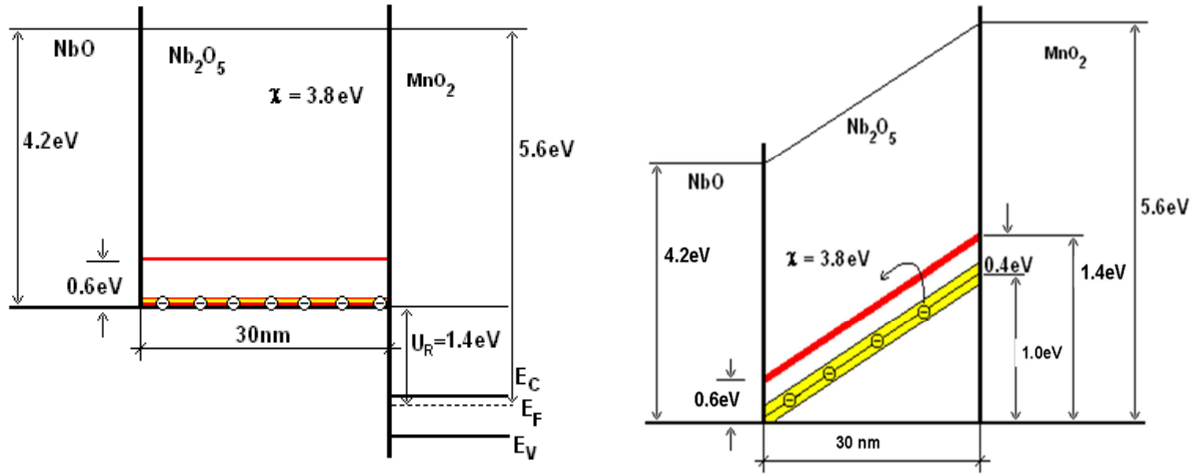


*Fig.2. and 3. MIS structure model for NbO capacitors before (left) and after (right) thermodynamic equilibrium*

Interface between NbO and Nb<sub>2</sub>O<sub>5</sub> is not ideal. It is supposed that there is an interface layer with thickness 2-5 μm, which is formed by a stable oxide NbO<sub>2</sub> and concentration of oxygen atoms gradually increases from NbO anode to dielectrics.

Vacancies and interstitials in the dielectrics act as localized states and create an interface dipole layer. Dipole moment of the layer changes the barrier between MnO<sub>2</sub> cathode and Nb<sub>2</sub>O<sub>5</sub> dielectrics. This interface layer is responsible for potential barrier dispersion. Dipole moment causes, that the potential gradient is reduced at the interface NbO – Nb<sub>2</sub>O<sub>5</sub>, as it is shown on Fig.4.

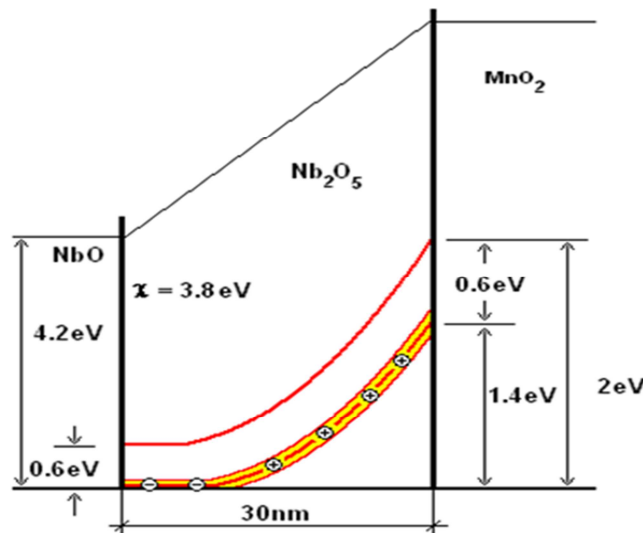


*Fig.4. MIS structure of NbO capacitor in thermodynamic equilibrium with dipole moments*



## 2.4 CARRIER TRANSPORT MECHANISM

A MIS structure model has been successfully applied to interpret the V-A, I-t or CV characteristics and their temperature or voltage dependences.

### 2.4.1 V-A characteristics

Dependence of leakage current  $I$  on applied voltage  $U$  in NbO capacitors in **normal mode** consist of three components:

$$I = G_o \cdot U + G_P \cdot U \cdot \exp(\beta_P \cdot U^{1/2}) + G_T \cdot U \cdot \exp(h/U) \quad (1)$$

- **Ohmic component.** Carriers move directly from one trap to the next one by tunnelling. Conductivity  $G_o$  in the impurity band can be expressed by similar formula as ohmic conductivity. This mechanism typically controls the VA characteristic in the voltage range below 0.5V.

- **Poole Frenkel component.** Poole Frenkel mechanism occurs by thermal emission from the impurity band to the conductive band over the locally reduced barrier in proximity of a Coulomb-attractive centre by applied electric field. It causes lowering of thermal ionization energy of such centre (Fig.5). Poole-Frenkel conductivity  $G_P$  is proportional to the carrier concentration, and the constant  $\beta_P$  is for Poole-Frenkel emission constant given by the formula

$$\beta_P = (e^3 / \pi \epsilon_0 \epsilon_r d)^{1/2} / kT. \quad (2)$$

The Poole Frenkel mechanism is dominant at typical application voltages and temperatures. Current is controlled by bulk processes in the insulating layer.

- **Tunneling component.**  $G_T$  and  $U_0$  are tunnelling current constants. The constant  $U_0$  is given by formula

$$U_0 = (8\pi\sqrt{2m^*} / 3eh)(e\Phi_{SI})^{1.5}t_0, \quad (3)$$

where  $m^*$  is effective mass of electron,  $h$  is Planck constant,  $e\Phi_{SI}$  is energy of the barrier between semiconductor and insulant, and  $t_0$  is the barrier thickness (Fig.5). Tunnelling current is dominant at very low temperatures and above rated voltage, which corresponds to electric field intensity  $> 200\text{MV/m}$ .

Charge carrier transport in **reverse** mode is given by thermionic emission of electrons from anode. The V-A characteristics is composed of stationary current, ohmic and Schottky components:

$$I = I_{ST} + G \cdot U + I_0 \cdot (\exp(\beta U) - 1) \quad (4)$$

- **Stationary current component** -  $I_{ST}$  is related to non-stationary measurement method and may be caused by ionic diffusion or polarization.
- **Ohmic component** - conductivity  $G$  behaves at low electric fields according to ohmic law and it can be expressed as

$$G = en\mu A/d, \quad (5)$$

where  $n$  is number of electrons,  $\mu$  is electron mobility in the dielectrics,  $A$  is dielectric's surface and  $d$  is dielectrics thickness.

- **Schottky component** is dominant for medium voltage. Leakage current is controlled by Schottky barrier. Schottky effect is the image-force reduction of the barrier potential for charge carrier emission when electric field is applied (see *Fig.5.*). The Schottky barrier reduction is

$$\Delta\phi = \left( \frac{e^3 U}{4\pi d \epsilon_0 \epsilon_r} \right)^{1/2} = \beta_s U^{1/2}, \quad (6)$$

Leakage current is then given by formula

$$I = I_0 \cdot \exp(\beta_s U^{1/2} - 1). \quad (7)$$

Saturation current of Schottky barrier  $I_0$  can be expressed as

$$I_0 = ART^2 \exp(-e\Phi_{IS}/kT), \quad (8)$$

where  $R$  is Richardson constant,  $k$  is Boltzmann constant,  $T$  is absolute temperature.

- **Diffusion voltage  $U_D$**  is voltage needed to overcome the potential barrier between  $NbO$  and  $Nb_2O_5$ . It can be obtained from diffusion voltage by

$$I_{Tresh} = ART^2 \exp(-e\Phi_{IS}/kT) \quad (9)$$

Conductivity modes are separated in *Fig. 6*. For  $U < U_D$ , current is controlled by  $MnO_2$ – $Nb_2O_5$  interface barrier. Diffusion potential barrier disappears for voltage higher than  $U_D$ . The second barrier between  $NbO$  -  $Nb_2O_5$  and the voltage drop on isolating  $Nb_2O_5$  layer play dominant role in electric current transport.

For  $T < 200K$ , Poole-Frenkel and Schottky mechanisms are negligible and tunnelling is a dominant mechanism. V-A characteristics in normal and reverse mode are identical. The measurements provide important information about carrier

concentration in the impurity band, height of potential barriers between anode, dielectrics and cathode and product of dielectrics thickness and dielectric constant.

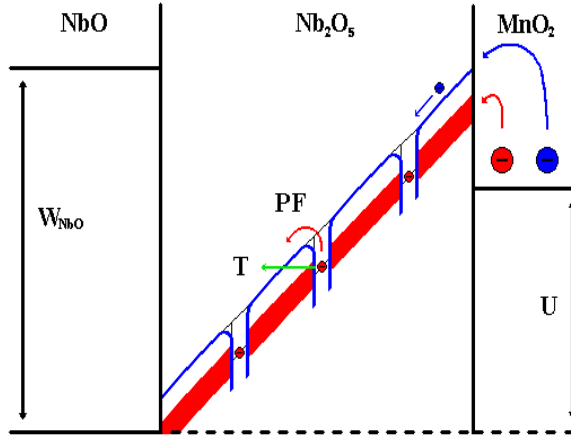


Fig.5. Schematic illustration of Poole-Frenkel and tunnelling emission

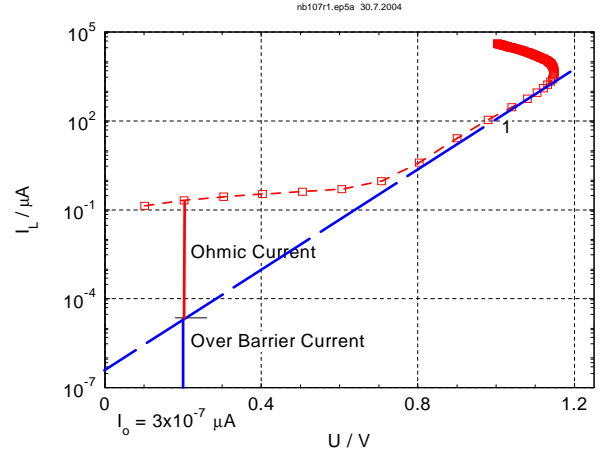


Fig.6. V-A characteristics of sample NbO300 in reverse mode

#### 2.4.2 Potential barriers and capacitance

Remarkable increase of capacitance in reverse mode is observed for NbO capacitors due to the potential barrier existence. There exists a depleted layer in Nb<sub>2</sub>O<sub>5</sub> near to the interface with MnO<sub>2</sub> layer, where the majority carrier concentration is lower than in bulk material. When acceptor concentration  $N_A \gg$  donor concentration  $N_D$ , the square of inverse capacitance  $C$  is given by formula

$$\frac{1}{C^2} = \frac{2}{A^2 e \epsilon_r \epsilon_0 N_D} (U_D + U), \quad (10)$$

where  $U_D$  is diffusion voltage. For  $U < U_D$ , the current is controlled by MnO<sub>2</sub> – Nb<sub>2</sub>O<sub>5</sub> interface barrier. Potential of MnO<sub>2</sub>–Nb<sub>2</sub>O<sub>5</sub> interface barrier (Fig.7.) and donor concentration  $N_D$  can be determined from the CV characteristics.

#### 2.4.3 Activation energy of leakage current

In normal conditions, only Poole-Frenkel mechanism is influenced by temperature. Total leakage current can be expressed by two components

$$I_L = I_{01} e^{-E_{a1}/kT} + I_{02} e^{-E_{a2}/kT}, \quad (11)$$

where  $E_{a1}$  represents activation energy of impurity band, and  $E_{a2}$  corresponds to Schottky mechanism limited by the interface Nb<sub>2</sub>O<sub>5</sub> – MnO<sub>2</sub>.

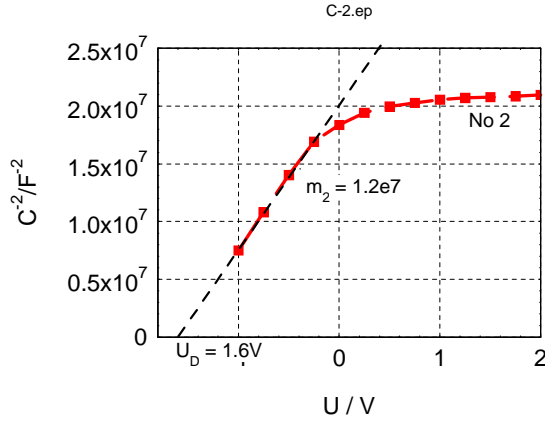


Fig.7. Diffusion voltage estimation from the C-V characteristics

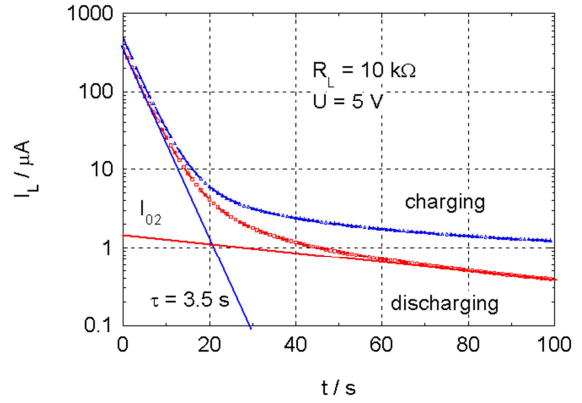


Fig.8. Leakage current vs. time in normal mode during capacitor charging and discharging

#### 2.4.4 Fast and slow energy localized states

Potential distribution in dielectric layer of NbO capacitors during charging and discharging is time dependent due to existence of fast and slow energy localized states with time constants  $\tau_1$  and  $\tau_2$ . In normal mode the fast charges are distributed at the electrodes (NbO and MnO<sub>2</sub>). Leakage current vs. time in normal mode during capacitor charging and discharging is shown in Fig.8. Discharging current of the capacitor after short-circuiting can be then described by

$$I_d(t) = I_{01}\exp(-t/\tau_1) + I_{02}\exp(-t/\tau_2) \quad (12)$$

Charging current is composed of three components:  $I_{01}$  – fast,  $I_{02}$  – slow and  $I_{ST}$  – stationary current component.

$$I_c(t) = I_{01}\exp(-t/\tau_1) + I_{02}\exp(-t/\tau_2) + I_{ST} \quad (13)$$

The I-t characteristics provide information about localized states in dielectric and their relaxation time.

#### 2.4.5 Noise

Noise in M system has its origin in the current fluctuations in the amorphous dielectric layer, in the contact system and at the interfaces. Voltage fluctuation can be characterized in frequency domain by application of the Fourier transformation on the voltage fluctuation measurement in time domain. This parameter is called voltage noise spectral density  $S_U$ . It is given by

$$S_u = U_N^2/\Delta f, \quad (14)$$

where  $U_N$  is noise voltage measured in frequency band  $\Delta f$ . An example of the voltage fluctuation measurement in frequency domain is shown in Fig.9.

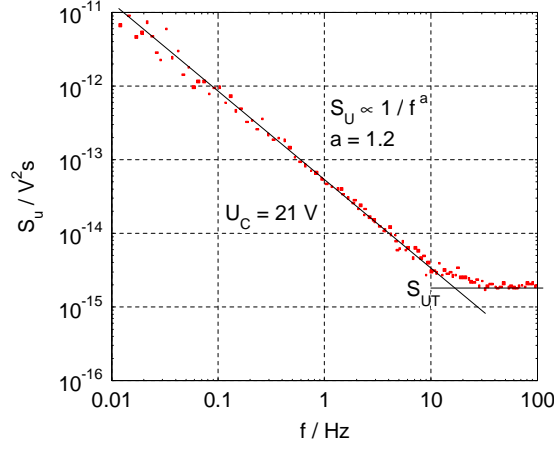


Fig.9. Voltage fluctuation in frequency domain

Voltage noise spectral density at low frequency is superposition of  $1/f^a$  noise caused by charge carrier trapping (G-R process,  $a=2$ ) or scattering on potential barriers (Shot noise,  $a=1$ ), burst noise caused by electron transport through cracks and thermal noise caused by random thermal movement of charge carriers.

Current noise spectral density measured in the frequency band  $\Delta f$  can be obtained from voltage noise spectral density measured on the load resistor  $R_L$ :

$$S_I = \frac{S_U}{R_L^2} (1 + \omega^2 R_L^2 C_X^2) = I^2 N / \Delta f, \quad (15)$$

where  $\omega$  frequency and  $C_X$  is capacitance of measured capacitor. The  $1/f$  noise spectral density can be expressed by generalized Hooge's formula

$$S_I = \alpha \cdot I^2 / f \cdot N, \quad (16)$$

where  $f$  is frequency,  $N$  is the number of carriers in the active region,  $I$  is current and  $\alpha$  is an empirical Hooge's constant, characterizing perfectness of the component structure.  $S_I$  is related to the technology. For good technology, it is proportional to the square of leakage current. It is however often related to the excess component of leakage current, when this dependence on leakage current is of higher power.

The component quality is then described by reliability indicator  $M_Q$ , which is defined as [19], [20]

$$M_Q = S_I / I^2 * f. \quad (17)$$

### 3. AIM OF DISSERTATION

The goal of this dissertation is to study and experimentally evaluate charge carrier transport in Nb<sub>2</sub>O<sub>5</sub> nanolayers in NbO capacitor, and on the basis of experimental data to propose optimization of the capacitors manufacturing process and consequences to the component reliability.

Main targets of the experimental part are summarized in following tasks:

- Study the charge carrier transport in NbO capacitors and define physical parameters, controlling leakage current
- Compare the charge carrier transport in NbO and Tantalum capacitors
- Verify the band diagram of MIS structure, find its basic physical constants
- Use the model and experimental results for analysis of NbO raw material
- Propose suitable dopants for NbO raw material improvement
- Optimize the anodic oxidation technology
- Study correlation of charge carrier transport parameters with component reliability and propose parameters for evaluation of quality of NbO capacitors

The measurements were done in the Czech Noise Research Laboratory at Brno University of Technology and AVX Czech Republic s.r.o., Lanškroun.

Following methods were used for measurement of charge carrier transport parameters:

- V-A characteristics in normal and reverse mode, at room temperature (300K) and at low temperature (78K)
- Capacitance of depleted layer with applied voltage in normal and reverse mode, its dependence on voltage and frequency
- Temperature dependence of leakage current
- Time dependence of leakage current during charging and discharging
- Noise spectral density in frequency and time domains for different voltages

The aim of the work is better understanding of transport mechanisms in the NbO capacitors and explanation of their unique properties. Target is to give complete overview of the new Niobium based component with highlighting strong and weak points of this technology. Basic study of raw material and anodic oxidation technology are the tools for better understanding driving forces which improve efficiency and reliability of NbO capacitors.

## 4. EXPERIMENTAL PART

### 4.1 STUDY OF BASIC PARAMETERS OF THE BAND DIAGRAM

#### 4.1.1 Tested samples

Tantalum, niobium and NbO capacitors from two manufacturers were used for the evaluation of transport parameters. Samples were prepared by different technology in order to see the effect of cathode material and production or influences of anodic oxidation. Procedures from 2.1 were used for capacitors production.

#### 4.1.2 Testing methods

Basic parameters of NbO capacitor were studied by methods described in 2.4.

- V-A characteristics in normal and reverse mode
- Capacitance of depleted layer
- Temperature dependence of leakage current
- Time dependence of leakage current during charging and discharging
- Noise measurement

#### 4.1.3 V-A characteristics

V-A characteristics of NbO capacitors with different *dielectric's thickness* (samples NbO100, NbO200 and NbO300) were measured in quasi-stationary and discharging mode after deep localized states charging separation.

#### 4.1.4 V-A characteristics in reverse mode

Leakage current is determined by potential barriers height at the interfaces of NbO–Nb<sub>2</sub>O<sub>5</sub> and Nb<sub>2</sub>O<sub>5</sub>–MnO<sub>2</sub>. Barriers were determined from V-A characteristics in reverse mode using (8). Leakage current at  $U > 0,5V$  is given by emission over the potential barrier Nb<sub>2</sub>O<sub>5</sub> – MnO<sub>2</sub>. Threshold voltage  $U_M$  was in range 0,7-1,2V, the potential barrier on interface Nb<sub>2</sub>O<sub>5</sub> – MnO<sub>2</sub>  $e\Phi_{IS} = 0.4$  to 0.6 eV. Band diagram of NbO capacitor  $B100\mu F/1,8V$  derived from measured V-A characteristics in reverse mode is schematically described in *Fig.10*.

#### 4.1.5 Fitting of V-A characteristics

**V-A characteristics** of NbO capacitors **in normal mode** were fitted with theoretical curves using formula (1) and parameters of carrier transport mechanisms were calculated. For  $U < 0.5V$ , V-A characteristics of ensemble NbO100 (*Fig.11.*) can be fitted by linear curve describing Ohmic mechanism. At voltages 1-5V, Poole-Frenkel mechanism is dominant. Tunnelling mechanism appears at  $U > 5V$  and drives characteristics above 8V. Correlation of theoretical and real curves suggests that the conductivity mechanisms in NbO capacitors are similar to that in Tantalum ones. Thickness of dielectric layer was estimated from coefficients  $\beta_p$  and  $\beta_s$ .

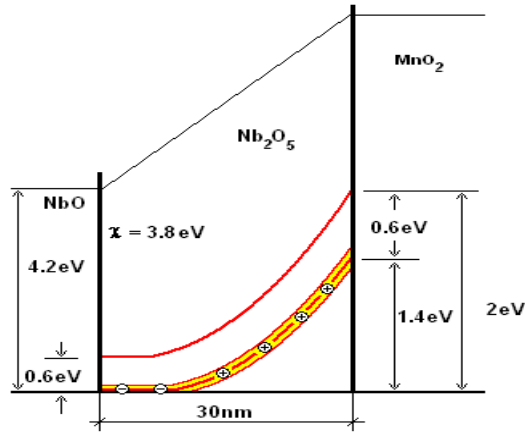


Fig.10. Potential barriers in NbO capacitor B100 $\mu$ F/1.8V without applied voltage

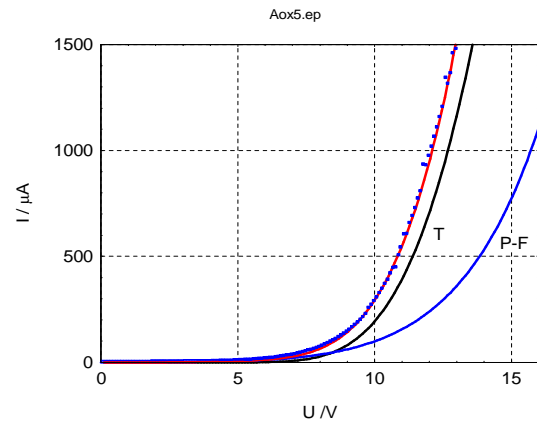


Fig.11. Fitted V-A characteristics (0-15V, linear scale)

Table 2. Experimentally determined vs real dielectric's thickness

Sample	C/ $\mu$ F	$U_R$ / V	$U_F$ / V	$\beta_P$ / $V^{-1/2}$	$\beta_S$ / $V^{-1/2}$	$d_P$ / nm	$d_S$ / nm	$d_F$ / nm
NbO 300	330/2,5	2,5	12	2,28	1,14	48	48	32
NbO 200	220/4	4	22	1,43	0,72	121	119	59
NbO 100	150/6,3	6,3	35	0,95	0,47	274	280	95

Formula (1) well describes V-A characteristics in normal mode and carriers are released from localized centres either by Poole-Frenkel / Schottky mechanisms or by tunnelling through potential barrier. The  $\beta_P$  decreases with the dielectric's thickness.

**V-A characteristics in reverse mode** for samples NbO100, NbO200 and NbO300 were fitted using formula (4). The values are summarized in Table 3.

Table 3. Fitted parameters for NbO100, NbO200 and NbO300 in reverse mode

Sample	$I_{ST}$ (nA)	$G_O$ ( $\mu$ S)	$I_0$ ( $\mu$ A)	$\beta$ ( $V^1$ )
NbO107	87	0,6	$1,7 \times 10^{-7}$	21
NbO203	230	0,74	$1,0 \times 10^{-8}$	25
NbO301	200	0,86	$1,5 \times 10^{-4}$	22



[illegible]

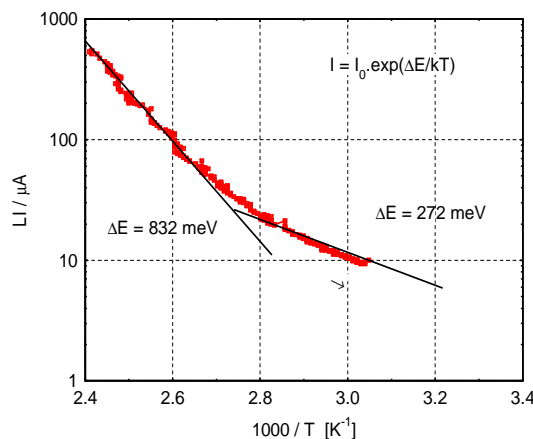
#### 4.1.6 Capacitance of depleted layer

Figure 1 is a plot of  $1/C^2$  versus  $U/V$  for Sample 1. The y-axis represents  $1/C^2$  in units of  $10^7$ , ranging from 0 to  $2.0 \times 10^7$ . The x-axis represents  $U/V$ , ranging from -1 to 2. The plot shows four data series for different temperatures: 25°C (blue circles), 55°C (green circles), 85°C (black triangles), and 105°C (red squares). The frequency  $f$  is 5 Hz. The curves show a linear increase in  $1/C^2$  with  $U/V$  for  $U/V > 0$ , and a non-linear decrease for  $U/V < 0$ . The slope of the linear region increases with temperature.

17

#### 4.1.7 Temperature dependence of leakage current

Leakage current vs temperature in both modes was measured on Ta and NbO capacitors with various dielectric's thickness and with MnO<sub>2</sub> or polymer cathode at rated voltage in temperature decreasing mode. Total leakage current can be expressed for all technologies by two components according to (11) – see *Fig.15*.



*Fig.15. Leakage current vs inverse temperature NbO– CP technology Y150/4*

The lower activation energy  $E_{a1}$  corresponds to the emission from impurity band. The band is shallow, independent on the anode and similar for the various thicknesses of dielectric. It has value 0,4eV for the MnO<sub>2</sub> and 0,2eV for conductive polymer technology. This band is present in all samples and is caused by oxygen vacancies in the dielectric, which act as electron donors causing the niobium pent-oxide to be n-type semiconductor.

The second activation energy  $E_{a2}$  is determined by emission over Schottky barrier on the interface dielectric –cathode. This mechanism dominates at temperatures above 90°C and has broader dispersion across the samples and technologies. Typical value of the second activation energy is 0.8eV for all technologies, but there are samples with activation energy up to 1.4eV. Some capacitors have the second activation energy similar to the first one. It indicates that the barrier height is not only a function of material, but can be influenced also by technology.

Activation energy of leakage current of NbO technology is very close to that of Tantalum one and energy band gap of Nb<sub>2</sub>O<sub>5</sub> is lower than of Ta<sub>2</sub>O<sub>5</sub> insulating layer. It can influence the leakage current and other temperature dependent characteristics.

#### 4.1.8 Time dependence of leakage current during charging and discharging

A typical dependence of leakage current vs. time in normal mode during capacitor charging and discharging is shown in *Fig.16*.

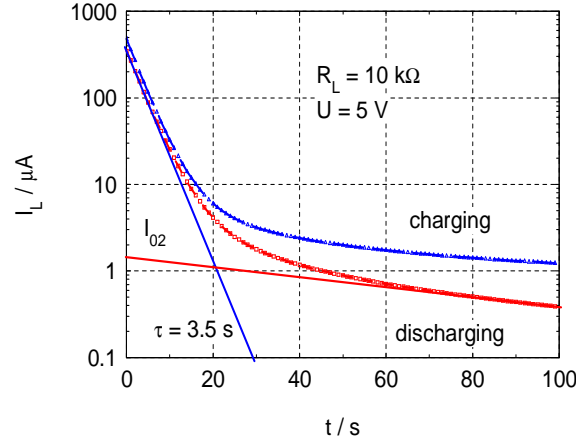


*Fig. 16. Leakage current vs. time in normal mode for NbO300*

The time dependence of leakage current during discharging can be fitted by superposition of two exponentials with relaxation constants  $\tau_1$  and  $\tau_2$ , using (12). The leakage current dependence is composed of fast and slow components, representing fast and slow charges in the system. The first relaxation constant is  $\tau_1 = 3$  to 5 s, the second relaxation constant is  $\tau_2 = 10$  to 100 s.

Fast charges are distributed at the conducting electrodes (NbO and MnO<sub>2</sub>), slow charges from deep localized states are distributed in the space charge region of the Nb<sub>2</sub>O<sub>5</sub> insulating layer including interfaces. They are created by generation-recombination processes between electron-localized states and valence band in the amorphous insulating layer. The charge in slow states is about 10% of the charge in fast states. In reverse mode the fast charges are attracted to the electrode and the ratio between fast and slow states is  $10^3$ .

#### 4.1.9 Restoring voltage of NbO capacitors

Equivalent resistance and capacitance of slow states in the NbO capacitor D220/4 were calculated from the restoring voltage evolution in reverse mode after NbO capacitor discharging (Fig.17). The NbO capacitor was charged to -0.5 V. After discharging of slow states, the voltage  $U_M$  had value  $U_M = 13$  mV, which corresponds to capacitance of slow states  $C_2 = 5$   $\mu$ F. In normal mode at +0.5V,  $U_M$  after slow states discharging  $U_M = 28$  mV.

Maximum value of restoring voltage  $U_M$  depends on applied voltage and on insulation layer conductivity. The lower insulation layer conductivity the higher maximum restoring voltage was observed.

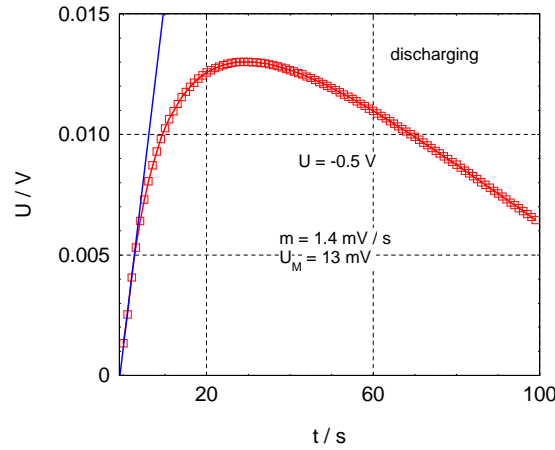


*Fig.17. Voltage evolution after discharging the capacitor NbO200 in reverse mode*

#### 4.1.10 Noise

A typical frequency dependence of voltage and current noise spectral density of NbO capacitor C100 $\mu$ F/4V in normal and reverse mode is in Fig.18 and 19. Noise at low voltages is  $1/f^\alpha$  type and is a superposition of shot and G-R noise. For high voltage, current noise spectral density is  $1/f$  type and is typical for tunnelling.

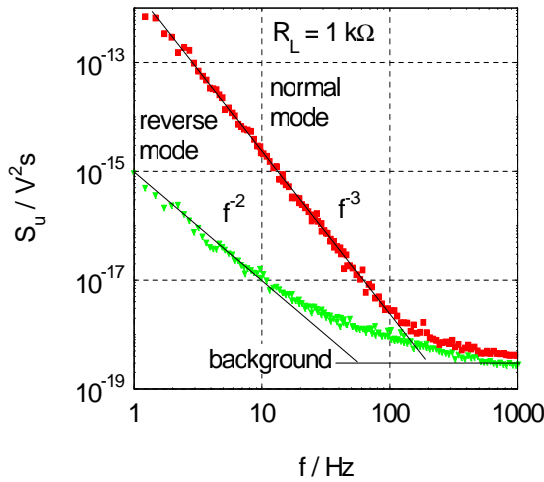


*Fig.18. Voltage noise spectral density vs. frequency in normal and reverse mode*

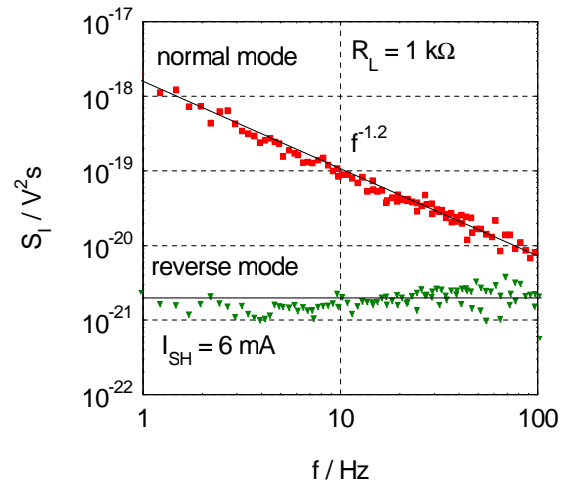


*Fig.19. Frequency dependence of current noise spectral density in normal and reverse mode*

The measurements showed that the noise sources of NbO capacitors are located similarly as for Tantalum capacitors [20] in the dielectric's layer and on the interface between the cathode and dielectric. Noise spectral density is given by superposition of white noise,  $1/f$  noise and generation-recombination noise. Occasionally the burst

noise is observed mainly in the reverse mode. In all samples the  $1/f$  noise is dominant in the low frequency range. Current noise spectral density has a quadratic dependence on leakage current, but often excessive component appears with quality indicator  $M_Q > 2$ . For high applied voltage where avalanche processes in dielectric are present the quality indicator  $M_Q$  is in range 2-6.

## 4.2 IMPROVEMENT OF THE TECHNOLOGY

### 4.2.1 Comparison of Nb and NbO technology

#### 4.2.1.1. V-A characteristics

To find more information about the current flow process, V-A characteristics were measured in normal and reverse mode (*Fig.20 and 21*). Leakage current is in the application voltage range controlled in both cases by Poole-Frenkel mechanism. The parameter  $\beta_p$  is slightly lower for Nb technology than for NbO technology. It means that effective dielectric's thickness for the Nb technology (NS1) was slightly lower, than for NbO technology (NA01) likely due to using lower forming voltage.

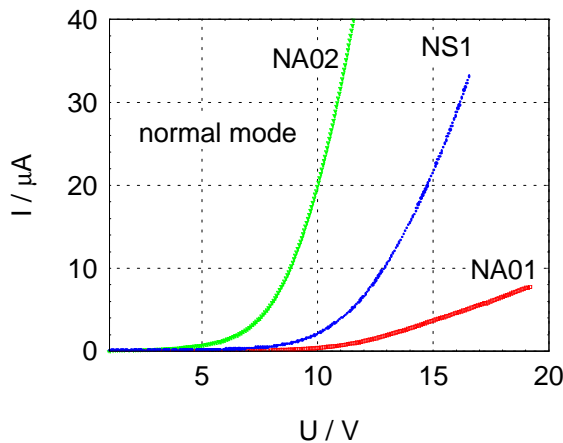


*Fig.20. V-A characteristics in normal mode for Nb and NbO technology*

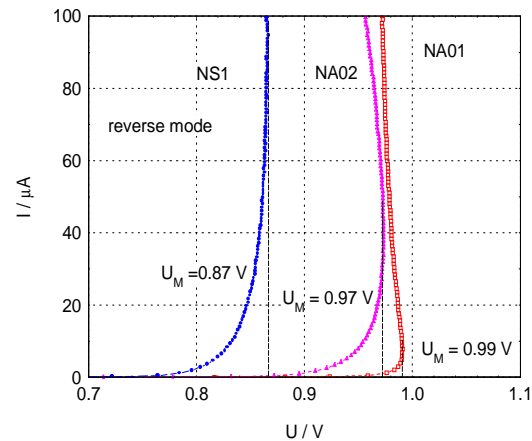


*Fig.21. V-A characteristics in reverse mode for Nb and NbO technology*

#### 4.2.1.2. Band diagram

V-A characteristics in reverse mode at  $T = 300$  K, tunnelling current transport in normal and reverse mode at  $T = 80$  K and CV characteristics were used to determine potential barriers height of Ta, Nb and NbO capacitors. Difference of barriers on interface NbO –  $\text{MnO}_2$  is lower than that for Ta –  $\text{MnO}_2$ . That is why over barrier current component for NbO capacitor is higher than for Tantalum one.

Table. 4. Potential barrier height of Tantalum, Niobium and NbO capacitor

Capacitor	$E_{BMI}/eV$	$E_{BIS}/eV$
Ta	0,7 - 0,8	1,7 - 2,2
Nb	0,4 - 0,6	0,6 - 0,9
NbO	0,4 - 0,6	0,9 - 1,4

Higher leakage current of Nb and NbO capacitor is caused by lower potential barriers and higher number of defects in dielectric due to additional stable oxide.

## 4.2.2 NbO powders with various parameters

### 4.2.2.1 V-A characteristics

Capacitors D150 $\mu$ F/6.3V, D220  $\mu$ F/4V, and D330  $\mu$ F/2,5V were prepared from NbO powders with low or high specific surface and from three suppliers, which used different technology of Nb<sub>2</sub>O<sub>5</sub> reduction. One sample of lower CV/g NbO powder from HC Starck was doped with a dopant which is supposed to stabilize free vacancies in the dielectric. Current transport was evaluated via temperature dependences of leakage current in the temperature range -55/+125°C (Fig.23)

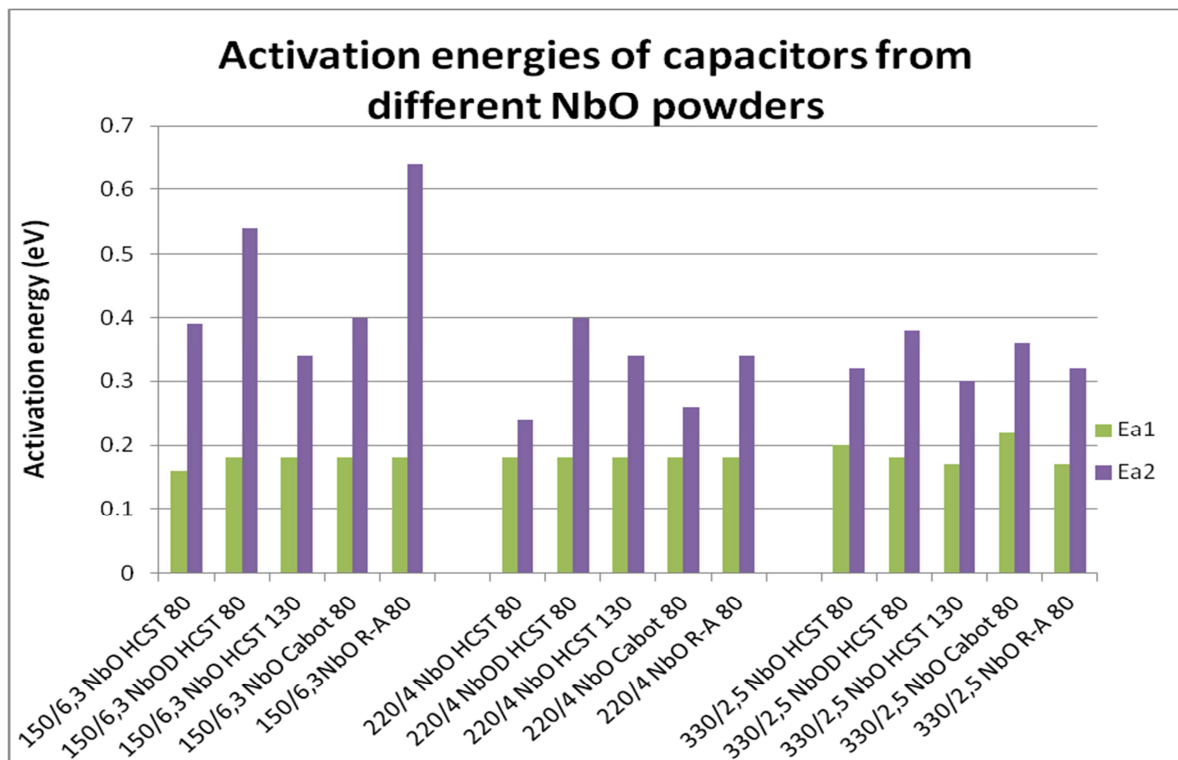


Fig.22. Activation energies of three types of NbO capacitors from different NbO powders

Activation energy  $E_{a1}$  is comparable for all five types of powders. It means that activation energy of impurity band caused by oxygen vacancies is independent on powder preparation. Activation energy  $E_{a2}$  is different for each powder ensemble. Doped powder has the highest  $E_{a2}$ , it means it has the highest barrier height between  $\text{MnO}_2 - \text{Nb}_2\text{O}_5$  insulating layer. The barrier height is the lowest for HCST 130k powder. The above mentioned data imply that the way of powder preparation is important for the proper barrier height formation.

#### 4.2.3 Stability of doped powder

The capacitor from 80k doped NbO powder was subjected to reliability tests. V-A characteristics before and after 2000 hours at 105°C and at 66% of rated voltage (10,6V) were compared (Fig.24 and 25).

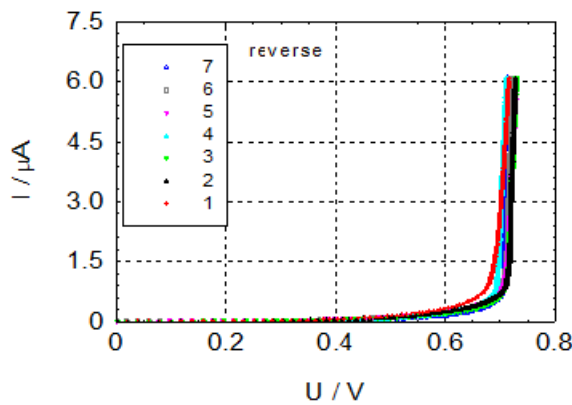


Fig.23. VA characteristics in reverse mode of doped samples NbD03 after ageing

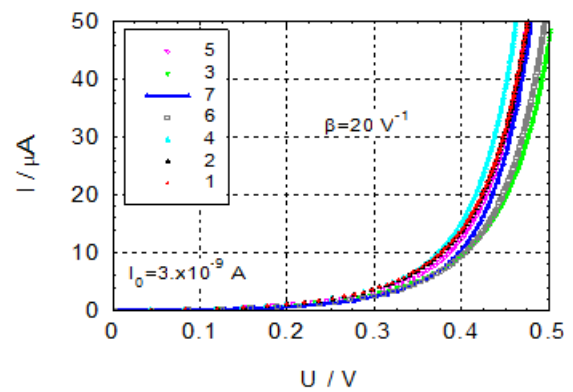


Fig.24. VA characteristics in reverse mode of non-doped samples NbZ03 after ageing

Diffusion voltage before ageing is similar for capacitors from both doped and un-doped powder. Diffusion voltage decreases after ageing, which means reduction of potential barrier between  $\text{Nb}_2\text{O}_5$  dielectric and  $\text{MnO}_2$  cathode. The diffusion voltage of capacitors from doped NbO powder had better stability after ageing, than in case of un-doped powder. Doping has positive effects on stability of effective thickness of dielectric after ageing and amount of oxygen vacancies in dielectric.

#### 4.2.4 Dielectric's cleaning

Defects are repaired by additional forming, but the forming process itself does not ensure fully uniform dielectric layer. Acid cleaning of the anode surface and thermal treatment at 300°C were used to improve dielectric created by the first forming.

Bake after 1<sup>st</sup> forming shows no improvement. Acid cleaning increases the threshold voltage and the potential barrier between Nb<sub>2</sub>O<sub>5</sub> – MnO<sub>2</sub>. It proves that the interface quality between the dielectric and MnO<sub>2</sub> cathode can be improved by the acid cleaning. Significant improvement of leakage current in normal mode is evident on the ensemble with the acid clean of the first dielectric. Achieved leakage current is approximately five times lower, because Poole-Frenkel and tunnelling conductivities are reduced. It indicates that number of defects in deep localized states is reduced by acid cleaning. Also barrier height between NbO and dielectric, calculated from the tunnelling component  $U_0$ , is higher for acid cleaned ensembles.

V-A characteristics clearly show that the acid cleaning of dielectric after 1<sup>st</sup> anodizing significantly improves both potential barriers and reduces number of defects in dielectric. Unlike standard leakage current measurement in one fixed time, the V-A plot gives complex information about the transport characteristics improvement.

#### 4.2.5 Anodic oxidation improvement

Effect of anodic oxidation parameters was studied by means of V-A characteristics in reverse mode at 300K, and by fitting of tunnelling current component of V-A characteristics at 100K. Anodizing current densities in the range 50-300mA, forming temperatures 22°C and 60°C and forming voltage 11-13V, resp. 24-28V were studied.

Effect of anodic oxidation parameters on potential barriers height was evaluated from V-A characteristics in reverse mode. Influence of anodizing current, electrolyte temperature and insulation layer thickness in reverse mode for capacitor B47μF/4V are shown on typical V-A characteristics on *Fig.26-28*, measured at 100 and 300 K.

Anodizing current has influence on reverse voltage  $U_{RM}$  and saturation current. Optimum anodizing current is around 150mA/g. Too high or too low anodizing current means lower threshold voltage and high saturation current. Low anodic current density leads to a crystalline structure. High anodic current density leads to high defects concentration. Threshold voltage  $U_{RM}$  increases and saturation current decreases also when anodizing voltage and anodizing temperature increases.

Both V-A characteristics at 300 K and at 100 K give good overview about the processes in the dielectric when anodizing parameters are modified. By properly selected anodizing parameters, the dielectric can be significantly improved. Improvement is caused by increasing of the insulation layer affinity, which can be explained by influence of the interface quality due to gradient of oxygen on the NbO-Nb<sub>2</sub>O<sub>5</sub> interface. It is supposed, that the oxygen vacancies create a thin dipole layer on the interface, which reduces the barrier height. Optimized anodizing



conditions reduce the defect concentration and increase the potential barrier on the interface. The effect is stronger for thinner insulation layer.

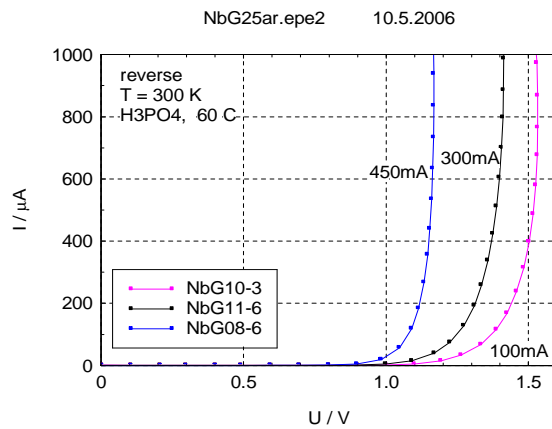


Fig.25. V-A characteristics in reverse mode for B47 $\mu$ F/4V and for different anodizing currents

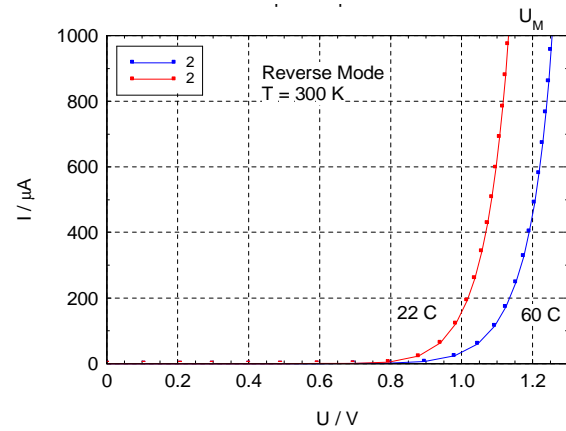


Fig.26. V-A characteristics in reverse mode for B47 $\mu$ F/4V and temperature of electrolyte 22°C, resp. 60°C

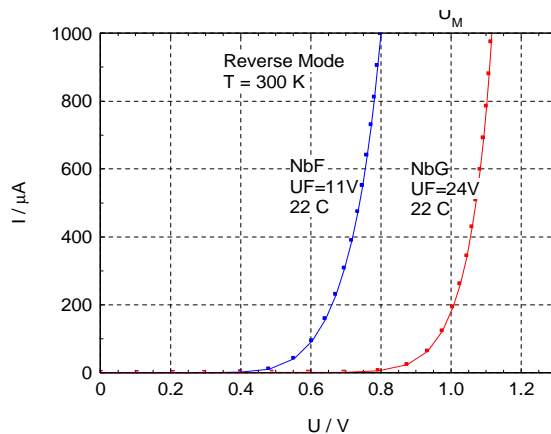


Fig.27. V-A characteristics in reverse mode for B47 $\mu$ F/4V and different anodizing voltages

#### 4.2.6 Correlation of transport parameters with reliability

Methods for reduction of the oxygen vacancies by improved anodic oxidation were studied by fitting of the VA characteristics to calculate the charge carrier transport constants, which were compared with the reliability of capacitors. VA characteristic constants were correlated to the mechanisms which are responsible for the reliability.

Six different technologies of anodic oxidation have been applied on 100 $\mu$ F/4V Niobium Oxide capacitor, formed at 11-13V. Defects in the dielectric were reduced by the dielectric's growth rate modification or by additives which reduce the charge mobility or by adding wetting agents. V-A characteristics were measured in voltage range 0-15V in quasi-static mode.

Capacitors prepared by 6 different anodizing technologies, were subjected to the accelerated ageing 2000hrs at 125°C and 0.66% rated voltage. Strong correlation of the leakage current change with the Poole-Frenkel conductivity has been found (Fig.28). Poole-Frenkel conductivity is proportional to the carrier density, i.e. oxygen vacancies concentration.

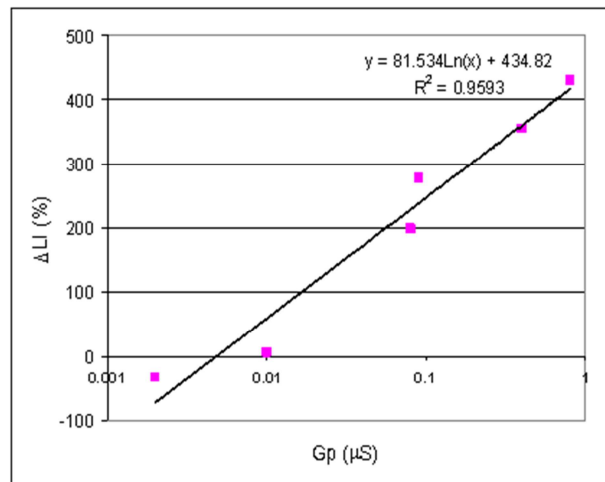


*Fig.28. Correlation of leakage current change after 2000hrs at 125°C and 66%Ur with the Poole-Frenkel conductivity  $G_p$*

The data show that after ageing no further conductivity mechanism appears and only existing parameters deteriorate indicating that numbers of oxygen vacancies are growing. The best technologies, which give relatively small or no change of leakage current after ageing, have the Poole-Frenkel conductivity  $G_P$  below 10nS. It implies that the Poole-Frenkel conductivity is a good indicator for component quality and the recommendation should focus on further technology improvement in terms of reduction of this particular conductivity mechanism.

## 5. CONCLUSIONS

Subject of this dissertation was to study and experimentally evaluate charge carrier transport in NbO capacitors, verify the model of band diagram of NbO-Nb<sub>2</sub>O<sub>5</sub>-MnO<sub>2</sub> MIS structure and use theoretical model and carrier transport analysis for optimization of the capacitors manufacturing technology and prediction of the component reliability.

Niobium oxide capacitor was described and compared to Tantalum capacitor. Key difference is that the anode is already oxidized and provides better resistance against burning. The second stable oxide (NbO<sub>2</sub>) is responsible for the additional self-healing effect, which reduces the short circuits, but creates additional impurity band in the dielectric.

Amorphous dielectric and its interface barriers with cathode and anode are described using MIS structure. In normal mode, leakage current is result of superposition of ohmic (low voltage), Poole-Frenkel (application voltages) and tunnelling (high voltage) mechanisms, in reverse mode Schottky emission appears. Threshold voltages in both normal and reverse modes are defined by the barriers on the interfaces between the dielectric and electrodes.

The NbO capacitors differ from Tantalum capacitors only by the parameters of its structure, not by the principles. Lower potential barriers and higher number of defects in the dielectric, caused by additional stable oxide, result in higher leakage current. Niobium capacitors have identical transport characteristics. Basic difference is in the quality of the dielectric layer at the anode interface.

Noise characteristics are similar for both technologies. Although the DC value of leakage current is higher in Nb/NbO technology, the fluctuating current component (noise) is about the same or less than that for tantalum, which means that reliability of Nb/NbO technology will be similar to tantalum.

Theoretical and practical results were used in evaluation of anode materials and anodic oxidation technology of Nb<sub>2</sub>O<sub>5</sub> dielectric. It was shown that anodic oxidation parameters can change the potential barrier height and improve the leakage current or threshold voltage of the capacitor.

Transport mechanism change of NbO capacitors during reliability tests at elevated temperature and applied voltage were studied. No new mechanisms were found after ageing of capacitors, but Poole-Frenkel conductivity caused by carrier concentration in the mobility band increased. The method can contribute to better prediction of the capacitors reliability. The results are supposed to be used in the production of NbO and in continuous effort of volume efficiency and reliability improvement of NbO capacitors.

## 6. LITERATURE

- [1] GILL, J., Basic Tantalum Capacitor Technology. [www.avx.com](http://www.avx.com)
- [2] Odinec, L.L., Anodnije okisnyje plenki, Petrozavodsk (1998)
- [3] Ahmed, C., Metals and Oxide Films, **1**,320 (1973)
- [4] Sikula, J. et al., Tantalum and Niobium Oxide Capacitors: Leakage current, Anodic Oxidation and Reliability, CARTS Europe, Barcelona (2007), pp.213-222
- [5] Sedlakova, V. et al., Anodic oxidation and capacitors restoring voltage of Ta and NbO capacitors, CARTS USA, Jacksonville, (2011), pp.111-124
- [6] Sita, Z. et al., Dielectric Improvements in NbO Capacitors, CARTS Europe, Barcelona 2007, pp.123-129
- [7] Massalski, T, Binary Alloy Phase Diagrams, ASM International, 2nd Edition, 1990
- [8] Zednicek, T, Tantalum and Niobium Technology Roadmap, <http://www.avx.com/docs/techinfo/tantniob.pdf>
- [9] Zednicek, T., New Tantalum Technologies: Tantalum Polymer and Niobium Oxide Capacitors, <http://www.avx.com/docs/techinfo/tantniob.pdf>
- [10] Sikula J. et all., Charge Carriers Transport and Noise of Niobium Capacitors, CARTS Europe, Nice, (2002), pp. 32-36
- [11] Sikula, J. at al., Conductivity Mechanisms and Breakdown Characteristics Of Niobium Oxide Capacitors, CARTS Europe, Stuttgart (2003), pp. 281-285
- [12] Sikula, J. et al., Charge Carrier Transport and Storage in NbO Capacitors, CARTS EUROPE, Nice (2004), pp.178-181
- [13] Sikula, J. et al., Transport and Noise Characteristics of Niobium Oxide and Tantalum Capacitors, CARTS Europe, Prague (2005), pp. 210-216
- [14] Sikula, J. et al., Niobium Oxide and Tantalum Capacitors: Quantum Effects in Charge Carrier Transport, CARTS USA, Orlando (2006), pp. 421-427
- [15] Sikula, J. et al, Niobium Oxide and Tantalum Capacitors: Leakage Current and M-I-S Model Parameters, CARTS USA, Albuquerque (2007), pp.337-345
- [16] Mott, N., and Davis, E., Elektronye processy v nekristallicheskich vescestvach. Moskva, (1974)
- [17] Sze, S.M., Physics of Semiconductor Devices, Wiley-Interscience, New York, (1981)
- [18] Mead, C. A. Phys. Rev. **128**, (1962), pp.2088-2093
- [19] Teverovsky, A. Reverse Bias Behavior of Surface Mount Solid Tantalum Capacitors; CARTS USA (2002), pp.105-123
- [20] Sikula, J. et al., Low Frequency Noise of Tantalum Capacitors, CARTS EUROPE, Copenhagen, (2001), pp. 81-84
- [21] Jones, B.K., Electrical noise as a measure of reliability in electronic devices, Advances in Electronics and Electron Physics, vol. 67, pp. 201-257(1994)
- [22] Vandamme, L.K.J., Noise as a diagnostic tool for quality and reliability of electronic devices, IEEE Transactions on Electron Devices, vol. 41, no. 11, pp. 2176-2187, Nov.1994

## Curriculum vitae

Name and surname: **Zdeněk Sita**  
Date and place of birth: 26.6.1961 Šternberk, Czech Republic  
Residence: Krátká 937, 563 01 Lanškroun, Czech Republic  
e-mail: [sitaz@seznam.cz](mailto:sitaz@seznam.cz)

### Education:

1986	Doctoral degree (RNDr.) – Solid State Physics
1980-1985	Mathematical-Physical Faculty of Charles's University, Prague, Solid State Physics - Physics of Semiconductors Thesis: Study of electron states in layer-like structure of $\text{Sb}_2\text{O}_3$
1975-1980	Gymnázium Šternberk

### Work experience:

2008-now	<b><i>EPCOS s.r.o., Šumperk</i></b> - 08-15 Product development manager
1994-2008	<b><i>AVX Czech Republic s.r.o., Lanškroun</i></b> - 01-08 Development manager - 95-01 Assembly engineering manager - 94-95 Assembly process engineer
1985-1994	<b><i>TESLA Lanškroun</i></b> - 91-94 Divisional marketing and purchase manager of Hybrid Circuits Department - 85-91 R&D engineer – development of thick film cermet pastes

## Abstract

Niobium oxide capacitor is a new type of passive components, which was developed to overcome basic disadvantages of Tantalum capacitors – limited ore source and burning failure mode. Similarly to Tantalum one, the niobium oxide capacitor can be described as a reverse MIS structure. V-A characteristics in normal and reverse mode at 77 and 300K, capacitance dependence of depleted layer on voltage and frequency, temperature and time dependence of leakage current and noise spectral density in frequency and time domains for different voltages were used to study charge carrier transport mechanisms in Nb<sub>2</sub>O<sub>5</sub> dielectric and to define physical parameters, controlling the leakage current.

Experimental data verified validity of proposed MIS structure band diagram and provided its key parameters. It was proven that the charge carrier transport in NbO capacitors is given by ohmic, Poole-Frenkel and tunnelling component in normal mode, and Schottky emission in reverse mode. Poole-Frenkel mechanism in normal mode and Schottky emission in reverse mode are dominant in the standard application voltage range. At high voltages, the tunnelling mechanism in normal mode determines breakdown voltage of the capacitor. In reverse mode, the barrier height between dielectric and anode determines resistance against thermal breakdown of the capacitor.

It was found that NbO and Ta capacitors have identical conductivity mechanisms. Specifics of NbO anode material are reflected only in different values of the band diagram parameters, not in the principles of charge carrier transport mechanisms. This explains basic difference between both capacitors, which is in the quality of the dielectric layer at the anode - dielectric interface. Lower potential barriers and higher number of defects in the dielectric, caused by additional stable oxide, result in higher leakage current of NbO capacitor. This effect has however no effect on reliability of the component.

Theoretical models and determined testing methods were used to select proper anode materials, to evaluate suitable dopants for NbO raw material improvement and to optimize the anodic oxidation technology. Charge carrier transport parameters were correlated with the reliability and on the basis of experimental data optimization of the capacitors manufacturing process was proposed.

Better understanding of transport mechanisms in the NbO capacitors gave complete overview of the new Niobium oxide based component with highlighting strong and weak points of this new technology, and provided tools for better understanding of driving forces which improve efficiency and reliability of NbO capacitors.

## Abstrakt

Kondenzátor na bázi oxidu niobu je novým typem pasívní součástky, jehož vývoj byl motivován snahou vyřešit hlavní nedostatky tantalového kondenzátoru – omezený zdroj tantalové suroviny a nebezpečí hoření při průrazu. Chování kondenzátoru na bázi oxidu niobu lze stejně jako u tantalového kondenzátoru popsat prostřednictvím reverzní MIS struktury. Pro studium mechanismu transportu nosičů nábojů v dielektriku  $\text{Nb}_2\text{O}_5$  a pro stanovení fyzikálních parametrů, které řídí zbytkový proud, bylo využito měření V-A charakteristik v normálním a reverzním módu při 77 a 300K, dále závislosti kapacity ochuzené vrstvy na napětí a frekvenci, teplotní a časové závislosti zbytkového proudu a spektrální hustoty šumu ve frekvenční a časové doméně při různých napětích.

Experimentální data potvrdila platnost navrženého pásového diagramu MIS struktury a poskytla jeho klíčové parametry. Bylo ověřeno, že transport nosičů náboje v NbO kondenzátorech je určen ohmickou, Poole-Frenkelovou a tunelovou složkou v normálním módu, a Schottkyho emisí v reverzním módu. V rozsahu standardních aplikačních napětí dominují v normálním módu Poole-Frenkelova emise a v reverzním módu Schottkyho emise. Při vyšších napětích v normálním módu určuje průrazné napětí kondenzátoru tunelový mechanismus. V reverzním módu rozhoduje o odolnosti vůči tepelnému průrazu kondenzátoru výška bariéry mezi dielektrikem a anodou.

Bylo zjištěno, že NbO a Tantalové kondenzátory mají stejný mechanismus vodivosti. Specifika NbO anody se projevují pouze v rozdílných hodnotách parametrů pásového diagramu, nikoliv v principech mechanismu transportu nosičů náboje. To vysvětluje základní rozdíl mezi oběma kondenzátory, který je v kvalitě dielektrické vrstvy na přechodu anody a dielektrika. Nižší potenciálové bariéry a vyšší počet defektů v dielektriku, který je způsoben dalším stabilním oxidem, má za následek vyšší zbytkový proud NbO kondenzátoru. Tento jev však nemá žádný vliv na spolehlivost součástky.

Teoretické modely a vybrané testovací metody byly použity k volbě vhodných materiálů anody, ke stanovení vhodných dopantů a k optimalizaci technologie anodické oxidace. Byla nalezena korelace mezi parametry transportu nosičů náboje a spolehlivostí, a na základě experimentálních dat byly navrženy optimalizace výrobního procesu kondenzátorů.

Lepší porozumění transportním mechanismům v NbO kondenzátorech umožnilo úplný popis nové součástky na bázi oxidu niobu. Byly zdůrazněny silné a slabé stránky této nové technologie a nalezeny nástroje pro optimalizaci procesů, které umožní vyšší spolehlivost a efektivitu NbO kondenzátorů.